Title
The Role of Metal Halides in Enhancing the Dehydration of Xylose to Furfural

Journal
ChemCatChem, 7(3)

ISSN
1867-3880

Authors
Enslow, Kristopher R
Bell, Alexis T

Publication Date
2015-02-01

DOI
10.1002/cctc.201402842

Peer reviewed

ChemPubSoc Europe

DOI: 10.1002/cctc.201402842

CHEMCATCHEM Full Papers

The Role of Metal Halides in Enhancing the Dehydration of Xylose to Furfural

Kristopher R. Enslow[a, b] and Alexis T. Bell*[a, b]

The dehydration of xylose yields furfural, a product of considerable value as both a commodity chemical and a platform for producing a variety of fuels. When xylose is dehydrated in aqueous solution in the presence of a Brønsted acid catalyst, humins are formed via complex side processes that ultimately result in a loss in the yield of furfural. Such degradative processes can be minimized via the in situ extraction of furfural into an organic solvent. The partitioning of furfural from water into a given extracting solvent can be enhanced by the addition of salt to the aqueous phase, a process that increases the thermodynamic activity of furfural in water. Although the thermodynamics of using salts to improve liquid–liquid extraction are well studied, their impact on the kinetics of xylose dehydration catalyzed by a Brønsted acid are not. The aim of the present study was to understand how metal halide salts affect the mechanism and kinetics of xylose dehydration in aqueous solution. We found that the rate of xylose consumption is affected by both the nature of the salt cation and anion, increasing in the order no salt $< K^+ < Na^+ < Li^+$ and no salt $< Cl^- < Br^- < I^-$. Furfural selectivity increases similarly with respect to metal cations, but in the order no salt $< I^- < Br^- < Cl^-$ for halide anions. Multinuclear NMR was used to identify the interactions of cations and anions with xylose and to develop a model for explaining xylose-metal halide and water-metal halide interactions. The results of these experiments coupled with ^{18}O-labeling experiments indicate that xylose dehydration is initiated by protonation at the C1OH and C2OH sites, with halide anions acting to stabilize critical intermediates. The means by which metal halides affect the formation of humins was also investigated, and the role of cations and anions in affecting the selectivity to humins is discussed.

Introduction

Furfural is a high value chemical that can be used to produce a wide range of commodity chemicals[1,2] and fuels.[3–6] At present, the industrial production of furfural is accomplished through the Brønsted acid-catalyzed hydrolysis of agricultural waste, a process that has a product selectivity of less than 60%.[2,7] Furfural can also be sourced from any biomass material containing hemicellulose, a biopolymer which can be hydrolyzed to its principle component, xylose.[8] The subsequent dehydration of xylose produces furfural, however, this reaction is accompanied by complex side reactions leading to humins, intractable condensation products that can greatly reduce furfural selectivity. One approach for minimizing the loss of furfural is in situ extraction. Recent studies have shown that furfural selectivities in excess of 85% can be achieved by extracting the furfural formed by Brønsted acid-catalyzed dehydration of xylose using a biphasic system consisting of water and 4-methylpentan-2-one (MIBK)[9] or water/DMSO (1:1 v/v) and MIBK/2-butanol (7:3 v/v).[10] The increased furfural selectivity is attributed to the removal of furfural from the aqueous phase, thereby minimizing the possibility for furfural to undergo self-resinification or react with xylose to form humins. It has also been reported that the addition of salt, such as metal halides, to the aqueous phase enhances the extraction of furfural from the aqueous phase into the organic phase as a result of the salt lowering the activity of water, consequently increasing the activity coefficient of the furfural.[11]

A question seldom addressed in previous studies is how dissolved salt affects the rate of xylose dehydration and/or the rate of humins formation in an aqueous phase. To the best of our knowledge, this subject has received very little attention. What is known is that dissolved metal halides enhance the yield of furfural obtained through the aqueous phase dehydration of xylose.[12] Notably, this work was performed with low substrate concentrations and high temperature (35 mM xylose, 200 °C), conditions for which entropic effects are expected to diminish condensation reactions that lead to the formation of humins.[2] The only explanation given for the observed effect of salt addition is that it enhances the formation of 1,2-enediol, an intermediate in the mechanism of xylose dehydration.[12] Thus, the effects of dissolved salts on the rates of xylose dehydration and humins formation are little understood.

The present study was undertaken with the aim of developing a more thorough understanding of the role of metal hal-

[a] K. R. Enslow, Dr. A. T. Bell
Energy Biosciences Institute
Energy Biosciences Building, 2151 Berkeley Way
Berkeley, CA 94704-1011 (USA)
E-mail: alexbell@berkeley.edu

[b] K. R. Enslow, Dr. A. T. Bell
Department of Chemical and Biomolecular Engineering
University of California
Berkeley, CA 94720-1462 (USA)

Supporting information for this article is available on the WWW under http://dx.doi.org/10.1002/cctc.201402842.

ides in the dehydration of xylose to furfural in aqueous solution. Multinuclear NMR spectroscopy was used to probe both the interactions of metal cations and halide anions with water and xylose. These studies were complemented by experiments utilizing ^{13}C labeling of the xylose anomeric carbon to probe isomeric distributions and ^{18}O labeling of the xylose ring oxygen to identify reaction pathway populations. The results of these investigations have led to a mechanistic understanding of the means by which metal halides alter the kinetics of Brønsted acid-catalyzed dehydration of xylose in aqueous solution as well as the influence metal halides have on the formation of humins.

Results and Discussions

Xylose dehydration in water

Shown in Figure 1 is the temporal evolution of products formed during HCl-catalyzed dehydration of xylose in water at 140 °C. Over the course of the reaction, furfural is observed as the primary identifiable product. The difference between the

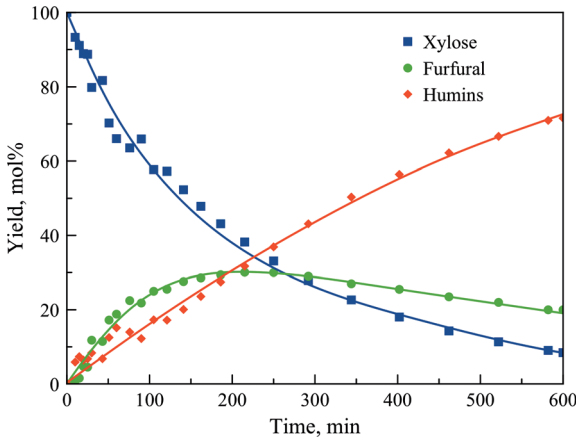

Figure 1. Dehydration of xylose (750 mM) at 140 °C catalyzed by HCl (200 mM) in water. Humins as presented represent the molar sum of soluble and insoluble degradation products.

consumption of xylose and the formation of furfural is attributed to the formation of humins—a combination of soluble (but not identifiable) products contributing to the discoloration of the reacting solution and a dark brown-to-black precipitate. During 600 min of reaction 92% of the xylose is consumed. The furfural yield increases initially, reaches a maximum of 30% after 200 min, and then slowly declines. By contrast, the yield of humins increases monotonically, and after 600 min constitutes the principal product of xylose dehydration.

At early reaction times (<10 min), xylose is consumed at a rate that exceeds the rate of furfural formation, suggesting the loss of xylose due to self-condensation or reaction with anhydro-xylose intermediates in addition to its dehydration to furfural. The decline in furfural yield for reaction times longer than that needed to reach the maximum yield suggests that furfural undergoes secondary reaction in the presence of a Brønsted acid. This hypothesis was confirmed by observing the reaction of an aqueous solution of furfural, containing 375 mM of furfural and 200 mM HCl, at 140 °C. After 2 h of reaction, the concentration of furfural decreased by 24% due to resinification (self-coupling), a process reported to occur readily at temperatures below 200 °C.[2] Furfural can also undergo condensation with anhydro-xylose intermediates via dioxolane-like bridging structures. Consistent with this proposal, it was observed (see Figure 2) that the addition of furfural at the start

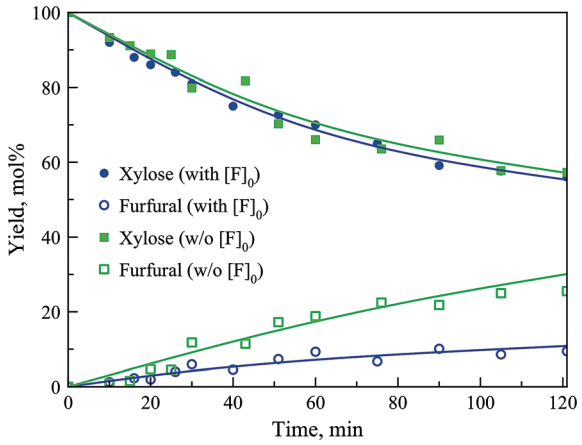

Figure 2. Dehydration of xylose (750 mM) at 140 °C catalyzed by HCl (200 mM) in water with and without an initial concentration of furfural ($[F]_0 = 400$ mM). Furfural yields shown only represent furfural produced directly from xylose, such that in the experiment starting with xylose and furfural, furfural yield = [total furfural] − $[F]_0$.

of xylose dehydration reduces the furfural produced from xylose (from 26 mol% to 9 mol%). However, direct condensation of furfural with xylose is unlikely, since the rate at which xylose is consumed is unchanged by the initial furfural concentration. These two observations indicate that a reaction occurs between furfural and an intermediate along the pathway from xylose to furfural. Scheme 1 shows a proposed pathway for the dehydration of xylose to furfural and for the loss of xylose and furfural via condensation reactions. The mechanisms by which the latter two processes might occur are given in Scheme 2 and 3.

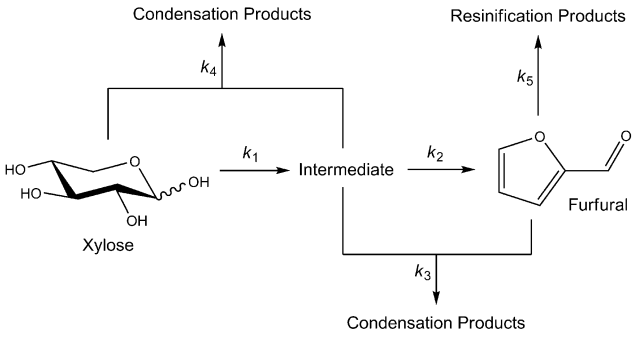

Scheme 1. A representative reaction pathway for xylose dehydration and degradation catalyzed by a Brønsted acid.

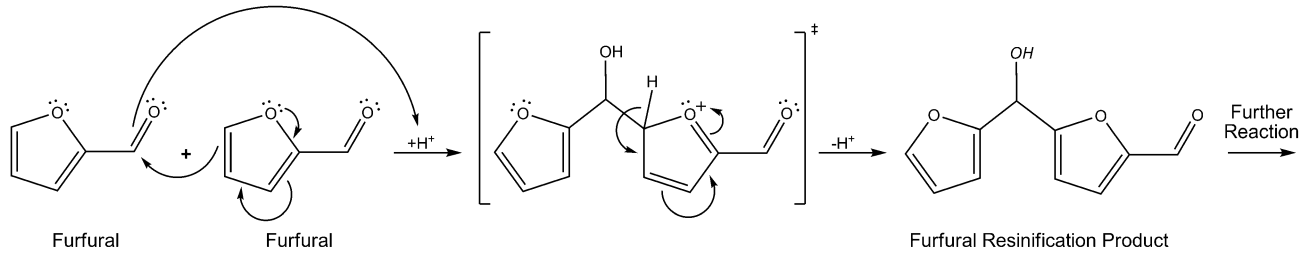

Scheme 2. A representative reaction pathway for furfural resinification via the coupling of two furfural molecules.

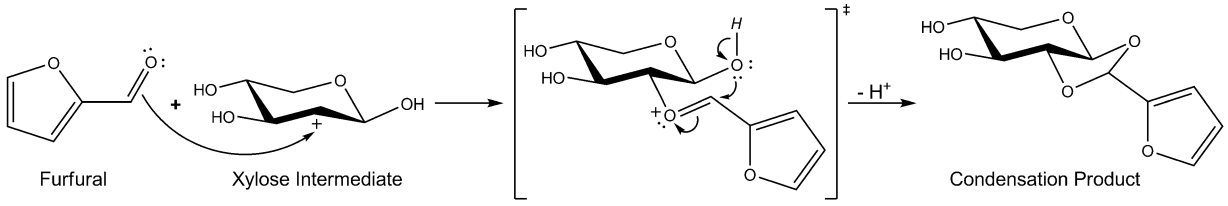

Scheme 3. A representative reaction pathway for furfural condensation with a xylose intermediate (mono-dehydrated at the C2 position).[2]

The kinetics of xylose consumption and furfural and humins formation can be described by the following set of ordinary differential equations [Eqs. (1)–(4)], which are based on Scheme 1:

$$\frac{d[X]}{dt} = -(k_1 + k_4[I])[X][H^+] \quad (1)$$

$$\frac{d[I]}{dt} = (k_1[X] - k_2[I] - k_3[I][F] - k_4[I][X])[H^+] \quad (2)$$

$$\frac{d[F]}{dt} = (k_2[I] - k_3[I][F] - k_5[F])[H^+] \quad (3)$$

$$\frac{d[H]}{dt} = (k_3[F][I] + k_4[X][I] + k_5[F])[H^+] \quad (4)$$

Here [X], [I], [F], and [H] are the concentrations of xylose, intermediate product, furfural, and humins, respectively. As the intermediates involved in the conversion of xylose-to-furfural were not observed, we can invoke the pseudo-steady-state assumption and set $d[I]/dt \approx 0$. Values for k_1, k_2, k_3, k_4, and k_5 were determined by least squares minimization of the residuals between the predicted concentrations of X, F, and H obtained by solving Equations (1)–(4), and the experimental data shown in Figure 1. The best-fit values obtained in this manner are $k_1 = 2.9(\pm 0.6)\times 10^{-4}\ L\,mol^{-1}\,s^{-1}$, $k_2 = 7.5(\pm 0.4)\times 10^{-4}\ L\,mol^{-1}\,s^{-1}$, $k_3 = 2.15(\pm 0.08)\times 10^{-3}\ L^2\,mol^{-2}\,s^{-1}$, $k_4 = 7.5(\pm 0.6)\times 10^{-4}\ L^2\,mol^{-2}\,s^{-1}$, and $k_5 = 1.0(\pm 0.1)\times 10^{-4}\ L\,mol^{-1}\,s^{-1}$. These results demonstrate that the rate coefficient for the consumption of intermediates produced from xylose is over twice as large as that for their production, and that humins are formed through condensation of furfural and intermediates involved in xylose dehydration at a rate that is more than twice as fast as the rate of condensation between xylose and the intermediates involved in xylose dehydration.

Xylose dehydration in the presence of metal halides

The effects of metal halides on the Brønsted acid-catalyzed dehydration of xylose in an aqueous solution were investigated using the chloride, bromide, and iodide salts of the monovalent metals lithium, sodium, and potassium. Each of these experiments was performed at 140 °C in a 5 M metal halide solution containing 50 mM HCl. The results of these experiments are presented in Figures 3–5.

Analysis of Figures 3A–5A reveals that xylose consumption occurs much more rapidly in brine than in water, the rate depending on the nature of both the cation and anion. For a given anion, the rate of xylose consumption increases in the following order: no salt $< K^+ < Na^+ < Li^+$. The initial rate of furfural formation increases in the same order, as can be seen from the data presented in Figures 3A–5B. In each case, the yield of furfural reaches a maximum and then declines with further reaction time, the time at which the maximum occurs decreasing as initial rate of furfural formation increases.

Initial rate data for xylose conversion and furfural formation is summarized in Table 1 for all metal halide solutions. The initial rates of both xylose consumption and furfural formation increase in the order no salt $< Cl^- < Br^- < I^-$. However, it is evident from Figures 3–5 that for longer reaction times the orders of Br^- and I^- are reversed. This change in order is attributable to the slow oxidation of iodide anions to molecular iodine in aqueous systems at elevated temperatures via a sequence of reactions that sum to the following stoichiometric reaction [Eq. (5)]:[13]

$$4\,I^- + O_2 + 4\,H^+ \rightarrow 2\,I_2 + 2\,H_2O \quad (5)$$

The occurrence of this reaction leads to a loss of both iodide anions and protons from solution and the formation of iodine. Evidence for this process was observed as a darkening of the

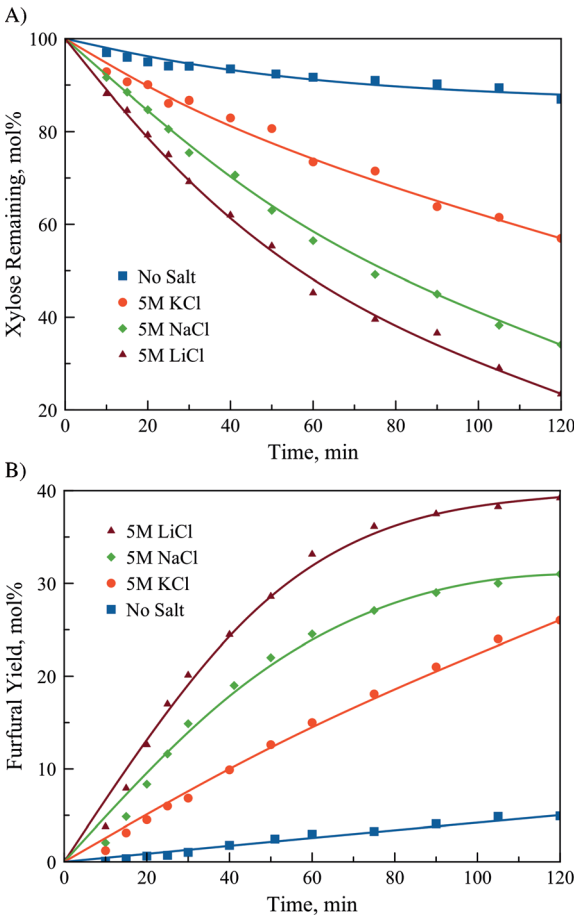

Figure 3. A) dehydration of xylose (750 mM) at 140 °C catalyzed by HCl (50 mM) in various 5 M metal chloride (aq) solutions. B) Resultant furfural formation.

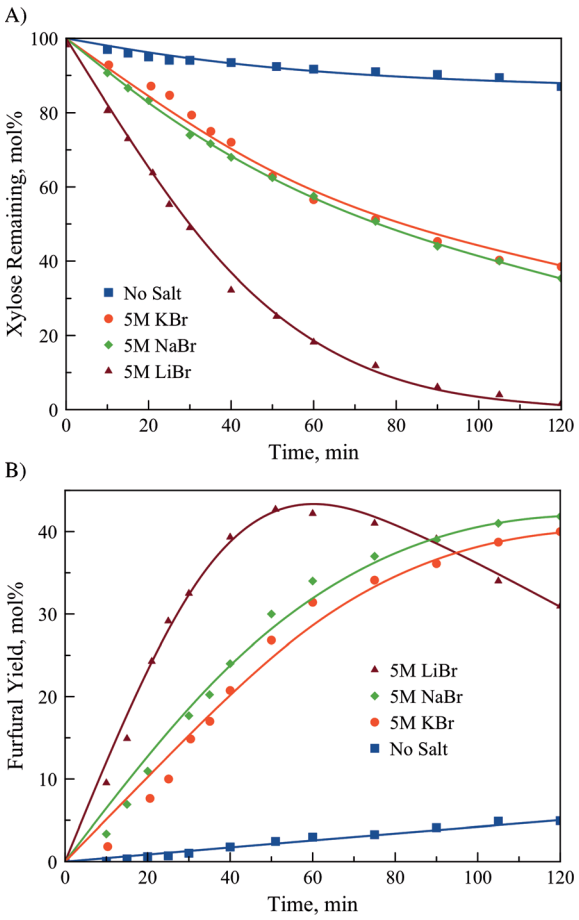

Figure 4. A) dehydration of xylose (750 mM) at 140 °C catalyzed by HCl (50 mM) in various 5 M metal bromide (aq) solutions. B) Resultant furfural formation.

Table 1. Initial rate of xylose (750 mM) dehydration and furfural formation at 140 °C catalyzed by HCl (50 mM) in various 5 M metal halide (aq) solutions.[a]

Salt	r_0, Xylose [μmol L^{-1} s^{-1}]	r_0, Furfural [μmol L^{-1} s^{-1}]	Furfural selectivity [%]
None	19.1	5.8	30.4
LiCl	156.3	69.3	44.3
LiBr	277.7	75.1	27.0
LiI	356.4	86.8	24.4
NaCl	91.3	38.6	42.3
NaBr	118.7	41.1	34.6
NaI	148.7	50.8	34.2
KCl	89.6	35.0	39.1
KBr	107.6	41.2	38.3
KI	126.3	48.8	38.6

[a] Includes furfural selectivity data for each salt. Data taken over the course of the first 5 min of each reaction.

reaction solution and a reduction in the rate of xylose dehydration. Further details of this process are discussed in the Supporting Information (Figure S2).

Table 1 also lists the selectivity toward furfural for each salt. In general, the furfural selectivity increases in the order $I^- \approx Br^- < Cl^-$, indicating that bromide and iodide anions may play greater roles in degradation reactions than do chloride anions. Notably, these selectivities are lower than those observed in Figures 3–5 due to an induction period that exists in the formation of furfural at short reaction times.

Effects of metal halides on the activity of water

The data presented in Figure 3–5 and Table 1 clearly indicate that the presence of metal halides strongly affects rate of xylose dehydration, as well as the formation of furfural and humins. To understand how halide salts affect these processes, we examined the effect of salt composition on the thermodynamic activity of water and the manner in which salt cations and anions interact with dissolved xylose.

The activity of water was determined for 5 M metal halide solutions using data taken from the literature.[14] The results, presented in Table 2, show that metal halides reduce the activity of water in the order no salt $> Cl^- > Br^- > I^-$ for a given cation and no salt $> K^+ > Na^+ > Li^+$ for a given anion. Comparison of these trends with the observed trend in the rate of xylose consumption reveals that the rate of xylose dehydration increases with decreasing water activity. This correlation can be attributed to the ability of metal halides cations and anions

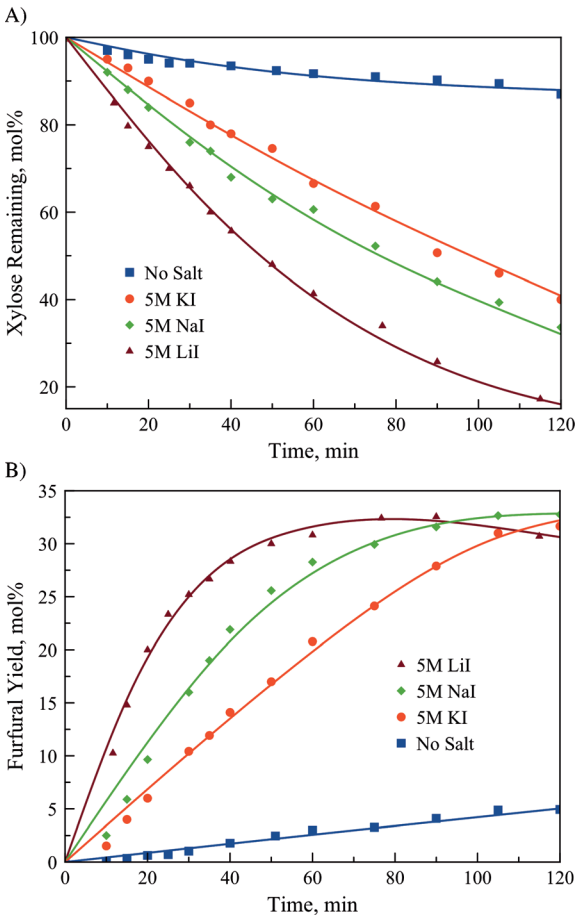

Figure 5. A) dehydration of xylose (750 mM) at 140 °C catalyzed by HCl (50 mM) in various 5 M metal iodide (aq) solutions. B) Resultant furfural formation.

Table 2. Molalities, salt activity coefficients, osmotic coefficients, and water activities of various 5 M metal halide (aq) solutions at 298 K.[13]

Salt	Salt molality [kg mol^{-1}]	Salt activity coefficient	Osmotic coefficient	Water activity
None	–	–	1	1
LiCl	5.593	2.404	1.748	0.703
LiBr	6.467	4.785	2.093	0.614
LiI	7.888	7.001	3.132	0.411
NaCl	5.595	0.939	1.238	0.779
NaBr	5.800	1.224	1.368	0.751
NaI	6.198	1.804	1.854	0.661
KCl	5.927	0.781	1.030	0.803
KBr	6.173	0.652	1.048	0.792
KI	6.635	0.734	1.097	0.769

to interact preferentially with water molecules, thereby reducing the interactions of water molecules with themselves or with other solute species. Such an interaction interrupts the hydrogen bond network within water, promoting a more stable restructuring of water around the metal halides.[15,16] This "kosmotropic" effect increases with ionic radius and/or charge, and can be estimated by the number of water molecules that hydrate each free ion (for example, 4 for K^+ and Na^+, 5 for Li^+, and to a lesser degree 1 for Cl^-/Br^- and 0 for I^-).[16] In the presence of strong kosmotropic species, water molecules are less able to interact with other solutes, and hence the activity coefficient of these solutes (such as xylose) increases, enabling them to interact more effectively with metal halide ions and protons. The latter effect is thought to enhance the extent of xylose protonation, as discussed in more detail below.

Effects of metal halides on the distribution of xylose conformers

Xylose in its crystalline form is present almost exclusively as α-xylopyranose; however upon dissolution in water it isomerizes to an equilibrium distribution of the five conformers shown in Scheme 4.[17] The distribution of xylose conformers was determined by ^{13}C NMR (see Figure S3 in the Supporting Information for peak assignments). As shown in Table 3, in the absence of acid and salt, only four of the five isomers are evident, the principal forms being β-xylopyranose (63.8%) and α-xylopyranose (35.6%). In 5 M salt solutions the ratio α-xylopyranose/β-xylopyranose increases slightly in the order $K^+ < Na^+ < Li^+$ for a given halide anion and in the order $Cl^- < Br^- < I^-$ for a given cation. Although lithium and sodium halide solutions increase the α-xylopyranose/β-xylopyranose ratio as compared to the case where no salt is added, potassium halide solutions promote marginally lower α-xylopyranose/β-xylopyranose ratios. Overall, the observed change in the ratio of α-pyranose/β-pyranose isomers of xylose in the presence of metal halides is smaller than that reported for isomers of ribose and galactose.[18,19] The larger effect of salts on these latter sugars is attributable to the presence of pyranose conformers containing axial-equatorial-axial (*ax.-eq.-ax.*) orientations of hydroxyl groups, for which the tri-oxygen core strongly attracts cations.

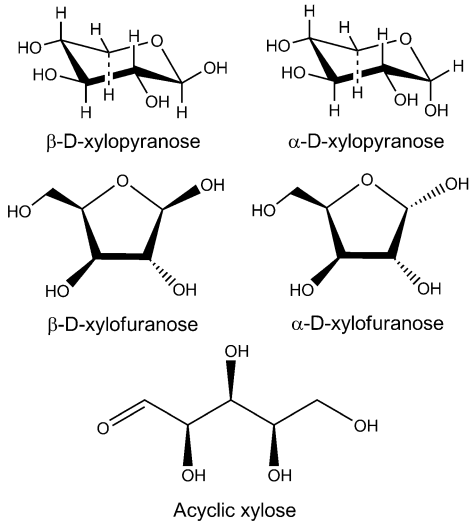

Scheme 4. The five isomers of xylose found after dissolving crystalline xylose in water.

Table 3. Xylose isomer distribution (%) of 1-^{13}C-xylose (750 mM) in D_2O (no salt), D_2O with 50 mM HCl (no salt w/50 mM HCl), and various 5 M metal halide (aq–D_2O) solutions as determined by measuring the ^{13}C NMR signals for the C1 carbons of individual xylose isomers.[a]

	Xylopyranose		Xylofuranose		Acyclic xylose
Salt	β-	α-	β-	α-	
None	63.8	34.2	1.2	0.8	–
None w/50 mM HCl	64.4	35.6	–	–	–
LiCl	63.1	36.9	–	–	–
LiBr	60.3	39.7	–	–	–
LiI	57.2	42.8	–	–	–
NaCl	63.0	37.0	–	–	–
NaBr	62.6	37.4	–	–	–
NaI	62.0	38.0	–	–	–
KCl	67.5	32.5	–	–	–
KBr	66.9	33.1	–	–	–
KI	66.8	33.2	–	–	–

[a] Dashes in place of numbers indicate that the isomer was not identified in solution. Data was recorded at room temperature after allowing 24 h to achieve an equilibrium distribution.

By contrast, the hydroxyl groups in β-xylopyranose are in *eq.-eq.-eq.* orientation and those in α-xylopyranose are in *ax.-eq.-eq.* orientation, and hence are less able to interact with cations. The distribution of xylose conformers reported in Table 3 was determined at room temperature. Previous studies have shown that the ratio of α-xylopyranose/β-xylopyranose in aqueous solutions increases with increasing temperature and, therefore, it is expected that this ratio will be higher at reaction temperature (140 °C) than at room temperature.[17]

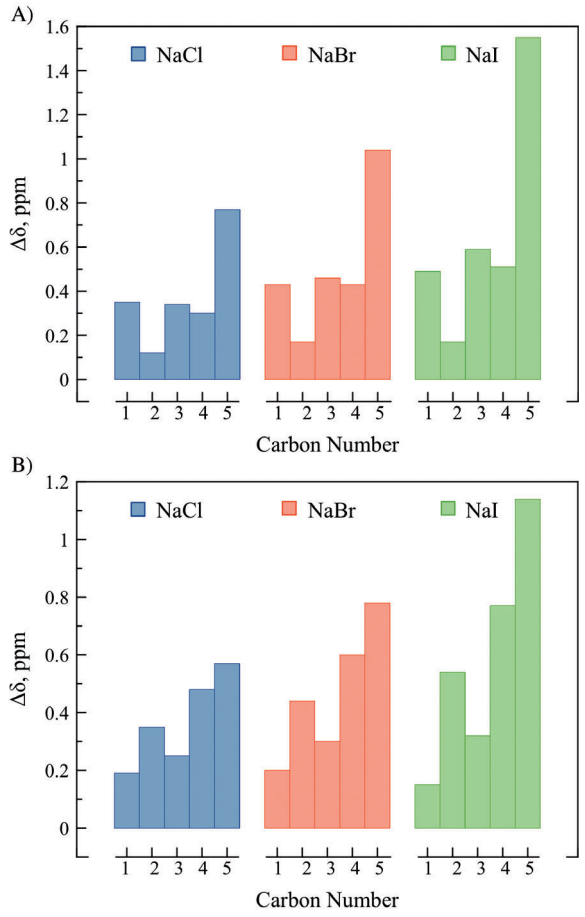

Figure 6. Dependence of chemical shift (Δδ) for each carbon of the α-xylopyranose A) and β-xylopyranose B) forms on halide anion for the sodium salts as determined by ^{13}C NMR analysis of 750 mM xylose in D_2O at 298 K in the presence of varying 5 M sodium halides.

Evidence for metal halide cation and anion interactions with xylose

^{13}C and ^{1}H NMR were used to observe the interactions of metal cations and halide anions with molecules of xylose dissolved in water. Evidence for these interactions was given by shifts in the positions of the ^{13}C NMR peaks or shifts in the ^{1}H NMR peaks for protons bonded directly to carbon atoms (proton chemical shifts for COH groups were not observed, owing to deuterium exchange with the D_2O solvent used to preserve the chemical nature of solution interactions). The observed changes in chemical shift ($\Delta\delta C_n$ and $\Delta\delta C_nH$) are presented in Tables S1 and S2 (in the Supporting Information). An example of the ^{13}C shifts observed for sodium halides is shown in Figure 6A and 6B for α- and β-xylopyranose, respectively. With a few exceptions $\Delta\delta C_n$ is positive for all carbons of both xylose conformers regardless of the metal halide composition, indicating the occurrence of electron deshielding at the carbon atoms. Each carbon is covalently bound to an oxygen atom that can interact with the metal cations in solution. These interactions withdraw electron density from the oxygen and in turn from the attached carbons, resulting in electron deshielding of the carbon nucleus. The metal cations interacting with the oxygen atoms of C–O–H groups are associated with the negative end of the dipole moment presented by these groups, whereas charge-compensating halide anions can associate with the positive end of the C–O–H dipole. The location of these anions is presumed to be close to the nearest hydroxyl proton given the steric barrier of such bulky ions nestling between the attached carbon and proton of the hydroxyl group. The cation–oxygen interaction withdraws electron density from carbon atoms of xylose, whereas the anion-proton interaction provides electron density. Given the charge density disparity between the cations and anions, the influence of the cations on shielding of carbon atoms is expected to dominate over the influence of anions, resulting in positive changes in carbon chemical shifts due to electron deshielding. However, as the anion associated with a given cation becomes larger, the anion becomes increasingly less effective in shielding the C–O–H group and the net deshielding effect of the cation–anion interaction with the sugar increases. This is precisely what is generally observed in Table S1 (Supporting Information)—as the charge density of the anion decreases, the magnitude of $\Delta\delta C_n$ increases, such that the change in chemical shift increases with respect to anion in the following manner: $Cl^- < Br^- < I^-$.

The interactions of metal cations with the ring oxygen atom have a qualitatively different effect from that observed for interactions of metal cation with C–O–H groups. While the

direct interaction between cation and ring oxygen is observed, as evidenced by positive values of $\Delta\delta C_5$ in all cases, the C5-O5-C1 dipole is aligned such that the positive end extends within the ring itself, prohibiting interaction with large halide anions. Consequently, the anion interacts with the cation on the periphery of the xylose molecule and consequently electron shielding of the C5 carbon atoms does not occur, and only the effects of the cation interaction with the ring oxygen are observed. This explains why the $\Delta\delta C_n$ is greater at the C5 position than at any other position. Furthermore, $\Delta\delta C_5$ increases with anion polarizability ($Cl^- < Br^- < I^-$), owing to the greater charge separation between a given cation and a more polarizable anion that affords a stronger dipole-ion interaction between the cation and ring oxygen. This effect, coupled with resonance effects from the nearby C4 carbon, can explain the trend in increasing values of $\Delta\delta C_5$ with respect to anion size.

Notably, for a given metal halide, $\Delta\delta C_n$ is always greater for α-xylopyranose than for β-xylopyranose at the C1 position, whereas the opposite is true at the C2 position. This trend is indicative of a stronger salt–sugar interaction at the C1OH group when xylose is present in the alpha form, whereas the interaction at the C2OH is strongest when xylose is present in the beta form. These differences have implications for the reaction mechanism, as discussed below.

The trends in $\Delta\delta C_nH$ shown in Table S2 (Supporting Information) follows the patterns observed for $\Delta\delta C_n$. For all protons, $\Delta\delta C_nH$ is positive and increases with respect to anion for a given cation in the following order: $Cl^- < Br^- < I^-$.

The interactions of chloride anions with xylose were probed by acquiring ^{35}Cl NMR spectra as a function of xylose concentration. Figure 7 shows that as the concentration of xylose increases, the width and the height of the chloride ion peak increase. These data can be used to determine the average number of Cl^- anions interacting with xylose using the following correlation [Eq. (6)]:[20]

$$\Delta\delta_{obs} = \Delta\delta_{free} + (\Delta\delta_{bound} - \Delta\delta_{free})N\frac{[xylose]_{\%}}{[NaCl]_{\%}}\frac{MW_{NaCl}}{MW_{xylose}} \quad (6)$$

For which: $\Delta\delta_{obs}$ = observed peak width of chloride ion, $\Delta\delta_{free}$ = peak width of chloride unbound to xylose, $\Delta\delta_{bound}$ = peak width of chloride bound to xylose, N = ratio of chloride ions to xylose molecules, $[NaCl]_{\%}$ = weight% of NaCl in solution, $[xylose]_{\%}$ = weight% of xylose in solution, MW_{NaCl} = molecular weight of NaCl, 58.44 g mol^{-1}, and MW_{xylose} = molecular weight of xylose, 150.13 g mol^{-1}.

By fitting Equation (6) to a plot of the measured values of the chloride ion peak width versus the weight percent xylose it was possible to determine a value of N. A value of $N \approx 3.8$ is determined, suggesting that every molecule of xylose interacts with ≈4 chloride anions or that each hydroxyl group interacts with one chloride anion.

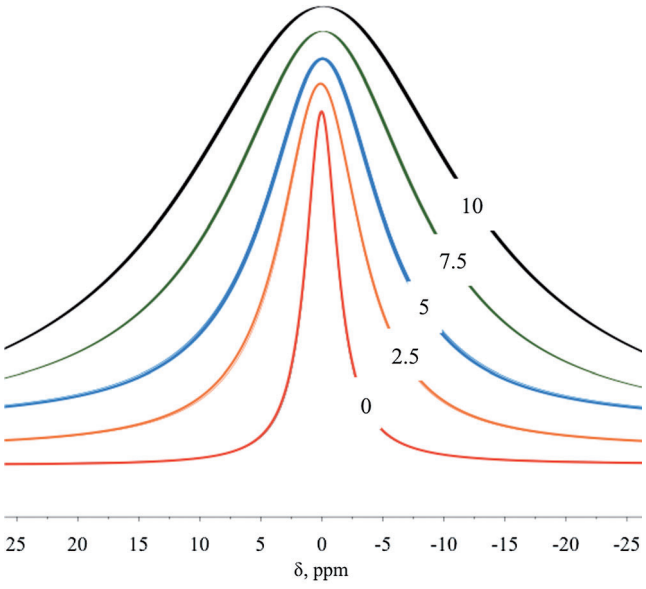

Figure 7. 1D ^{35}Cl NMR of the Cl^- peak of 5 M NaCl as a function of varying xylose concentration from 0–10 wt% in D_2O at 298 K.

^{18}O Isotopic labeling experiments

The NMR results presented in Table 2 show that the presence of lithium and sodium halides can cause a small increase in the ratio of α-xylopyranose relative to β-xylopyranose, and as noted earlier this ratio is expected to increase further when the temperature is raised from room temperature to the reaction temperature (140 °C). However, these changes do not appear to be sufficiently large to account for the significant effects of metal halides on the rates of xylose consumption and furfural formation presented in Figures 3–5. Therefore, it is more likely that these effects are attributable to specific interactions of metal cations and halide anions with molecules of xylose. Of particular note in this connection is the observation that cation and anion interactions are stronger with α-xylopyranose than with β-xylopyranose at the C1 position, whereas the opposite is true at the C2 position.

To further probe how metal halides affect the dehydration of α-xylopyranose and β-xylopyranose, experiments were performed with xylose labeled with ^{18}O-labeled at the ring oxygen position (D-[5-^{18}O]xylose]) both in the presence and absence of NaCl. At the end of reaction, furfural was extracted from the aqueous solution using toluene and then analyzed by GCMS to determine the location of ^{18}O in the furfural. The relative population of peaks at $m/z = 69$ versus 67 were used to determine whether ^{18}O in the xylose ring remained within the furan ring or transferred to the carbonyl group, respectively. In the absence of metal halides, 69% of the furfural produced contained ^{18}O within the furan ring and the remaining 31% contained ^{18}O in the carbonyl group. When the reaction was performed in 5 M NaCl, 52% of the furfural produced contained ^{18}O in the furan ring and 48% contained ^{18}O in the carbonyl group. The results of these experiments suggest that the interactions of Na^+ and Cl^- with xylose influence the mechanism and kinetics of xylose dehydration. The interpretation of these results is discussed in the next section.

Mechanism of xylose dehydration

Aqueous-phase dehydration of xylose to furfural catalyzed by a Brønsted acid can occur in one of two ways, initiated either by ring-opening to form the acyclic isomer of xylose followed by dehydration or by direct dehydration of either α- or β-xylopyranose. Experimental results have suggested that the Brønsted acid-catalyzed dehydration of xylose proceeds via the acyclic pathway,[21] however, theoretical studies of xylose dehydration suggest that pyranose ring opening followed by dehydration of the resulting aldose is less favorable energetically than direct dehydration of the pyranose ring followed by intramolecular rearrangement.[22] This study also shows that dehydration initiated at the C2OH position of xylopyranose is favored over that at the C1OH position, and that dehydration initiated at either C3OH or C4OH leads to fragmentation products rather than furfural. Hence, under the conditions investigated in this work, Brønsted acid-catalyzed dehydration of xylose in water with or without metal halides is presumed to proceed via either C1OH or C2OH dehydration, since fragmentation products were not observed.

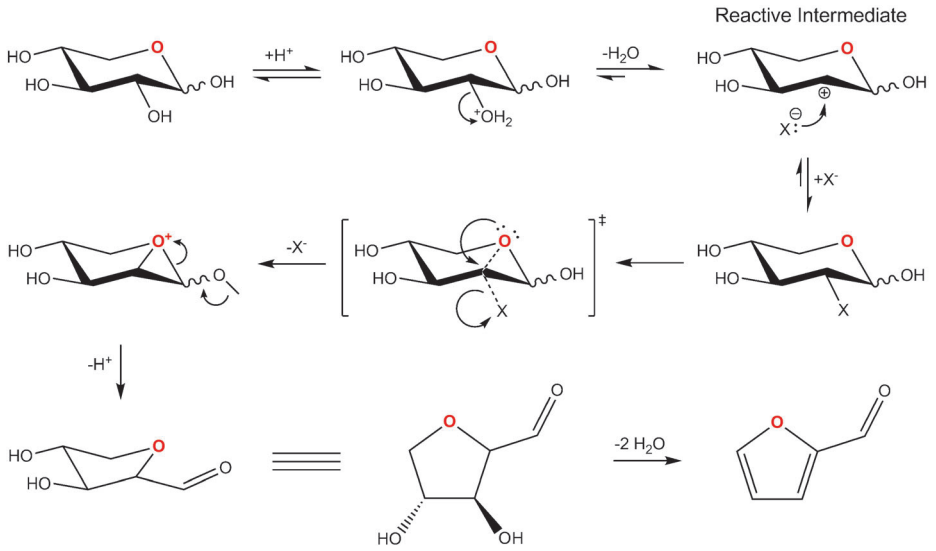

Scheme 5. The involvement of halide anions in stabilizing the carbocation formed during the initial dehydration of xylose at the C2 position.

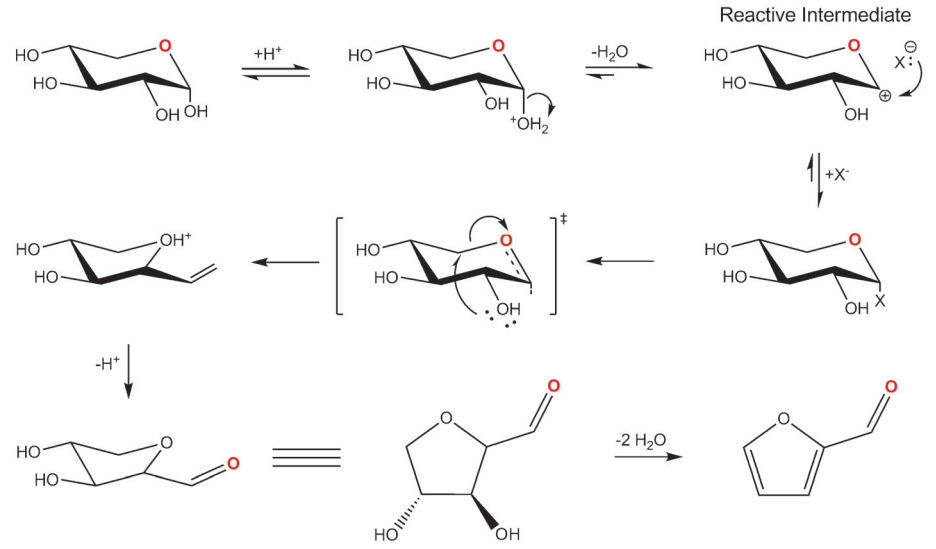

Scheme 6. The involvement of halide anions in stabilizing the carbocation formed during the initial dehydration of xylose at the C1 position.

When xylose dehydration is performed in the presence of metal halides, the metal cations can interact with the hydroxyl groups of the ring oxygen of xylose thereby increasing the C–OH and C-O–C bond lengths and lowering the energy necessary to break such C–O bonds. The use of a metal cation with strong kosmotropic character more effectively interrupts the xylose solvation shell, sterically hindering rehydration of the carbocation formed after dehydration. Moreover, halide anions can interact with the electronegative regions of xylose and stabilize any carbocations formed. The proposed influence of halide anions on Brønsted acid dehydration of xylose initiated at the C2OH and C1OH positions is presented in Schemes 5 and 6, respectively.

Scheme 5 shows the dehydration pathway proposed for xylose dehydration initiated by reversible protonation at the C2OH position of either α- or β-xylopyranose. This step is followed by the loss of water and the formation of a carbocation at the C2 position, which has been established in previous studies to be the rate-limiting step.[13] The carbocation is a reactive intermediate that can undergo rearrangement to form 2,5-anhydroxylose, which then further dehydrates to form furfural. The presence of a halide anion near the C2 carbon of the carbocation intermediate can aid in its stabilization and reduce the extent to which rehydration occurs at that position. As the halide nucleophilicity increases, so does the ability of the halide to stabilize the carbocations in protic solvents, i.e., $I^- > Br^- > Cl^-$.[13] This trend parallels that seen for the effect of halide composition on the rate of xylose dehydration (see Figures 3–5).

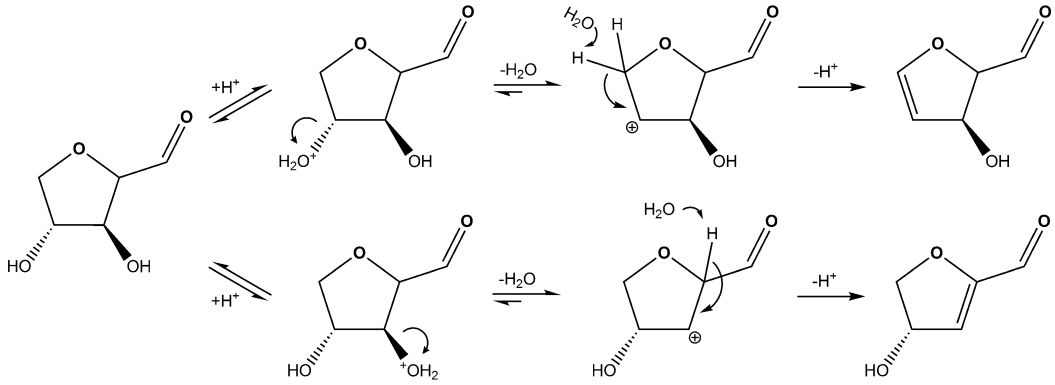

Scheme 7. The dehydration of 2,5-anhydroxylose at the C3 position (top) and C4 position (bottom), respectively.

Scheme 6 illustrates the proposed pathway for the xylose dehydration initiated by reversible protonation of the C1OH position of α-xylopyranose. As mentioned previously, dehydration of the β-xylopyranose conformer at the C2 position is more energetically favorable than at the C1 position, however, the α-xylopyranose conformer presents an anomeric hydroxyl group in the axial position. Hydroxyl groups in such positions are more easily protonated and removed as water than their equatorial counterparts. Therefore, both C1OH and C2OH initiated dehydration pathways are possible for α-xylopyranose. However, after the initial C1OH dehydration and the formation of the oxocarbinium cation, the next step requires the oxygen of the C2OH group to attack the C5 carbon. This step is expected to have a large energetic barrier because the equatorial C2OH must rotate around the plane of the xylose molecule and attack a carbon without formal charge. The addition of metal halides reduces this energetic barrier by not only elongating the C2-OH bond length allowing for increased mobility (via the metal cation-OH interaction), but also by increasing the partial positive charge on the carbon due to electron deshielding provided by the metal halide. Therefore, the salt–sugar interaction facilitates the production of furfural through the C1OH pathway by not only increasing the starting concentration of α-xylopyranose, but also by decreasing the barrier for ring reformation following the initial dehydration.

The results obtained from ^{18}O labeling experiments are fully consistent with the observed effects of metal halides on the pathways for xylose dehydration. In contrast to published results utilizing xylose-1-^{14}C that suggest the C1 carbon remains nearly completely at the aldehydic carbon of furfural,[21] ^{18}O labeling experiments indicate that the presence of metal halides can influence the final location of the C1 carbon and ring oxygen. Dehydration by means of protonation of the C1OH group, which results in the ^{18}O-labeled ring oxygen appearing in the furfural carbonyl group, occurs more rapidly than dehydration initiated through protonation of the C2OH group, which results in the ^{18}O-labeled ring oxygen remaining in the ring oxygen of furfural, when metal halides are present.

After primary dehydration at either hydroxyl group followed by ring rearrangement to form the 5-membered oxolane ring (2,5-anhydroxylose intermediate), furfural is formed via elimination of the hydroxyl groups at the C3 and C4 positions, as shown in Scheme 7. The ring structure is maintained throughout these final dehydrations because oxolane is very stable[23] and particularly resistant to attack by hydrolytic agents.[24]

The carbocationic intermediates produced during the dehydration of xylose can participate in condensation processes leading to humins. In the presence of metal halides the selectivity to furfural at initial reaction times decreased with increasing anion size, indicating that the ratio of the rates of condensation to dehydration increases with respect to anion in the order $Cl^- < Br^- < I^-$. As larger anions stabilize carbocation intermediates, they form longer, lower energy bonds with the carbon atoms that results in a less polar charge distribution between anion and carbocation. This effect lowers the partial positive charge on the carbon making it a weaker Brønsted acid that is less capable of participating in elimination reactions.[13] Together with the fact that larger anions are better leaving groups improves the probability that substitution occurs at the carbocation. Hence, although large anions promote the rates of xylose consumption and furfural production, such anions may also enhance the rate of promote more nucleophilic substitution and, consequently, lower selectivity to furfural.

Condensation reactions leading to humins can occur via a number of pathways involving either furfural or xylose and an intermediate involved in the dehydration of xylose. At the beginning of the Results and Discussion we showed that condensation involving furfural is preferred kinetically. Scheme 3 illustrates a possible mechanism for this process. In this example, xylose is substituted at the C2OH position by the nucleophilic carbonyl of furfural, followed by a nucleophilic attack on the carbonyl carbon by the C1OH oxygen, creating a furfural-xylose condensation product with a dioxolane bridge. The condensation of two furfural molecules (Scheme 2) can also be aided by the presence of metal halides. Furan resonance structures forming oxocarbenium ions can be stabilized by halide anions, allowing for the nucleophilic attack of a furfural C5 carbon on the carbonyl carbon of another furfural to form a di-furanyl resinification product.

Improving overall furfural yields

To this point, we have only discussed the effects of salt addition on the rate of xylose dehydration in aqueous solution and on the competing formation of humins. However, as noted in the Introduction, the yield of furfural can be enhanced by in situ extraction of furfural into a water-immiscible phase. For this reason, we end our discussion of the effects of salt addition by briefly examining the influence of NaCl on the dehydration of xylose performed in a two-phase water/toluene system. We note that the partition coefficient of furfural between a toluene phase and an aqueous phase (1:1 by volume) increases from 9 to 20 when 5 M NaCl is added to the aqueous phase (measured at 50 °C). Dehydrating xylose in such a biphasic system also improves the selectivity to furfural from 54 to 72% when 5 M NaCl (aq) was added to the aqueous phase (see Figure S6 in the Supporting Information). Thus, the addition of metal halides to a biphasic reaction system has the thermodynamic benefit of improving the efficacy of the extracting solvent relative to water

Notably, adjustments to reaction conditions can result in similar enhancements in selectivity. For example, lowering the metal halide concentration from 5 M reduces the difference between rate of xylose conversion and that of furfural production, resulting in increased selectivity (see Figure S1 of Supporting Information). The furfural selectivity can also be increased by increasing the temperature, which decreases the extent of side reactions and thereby increases the furfural selectivity, and at 200 °C approaches 100%.[2]

Conclusions

This study has shown that the addition of metal halides increases the rate of xylose dehydration in an aqueous phase catalyzed by a Brønsted acid. The enhancement in the dehydration rate is a function of both cation and anion composition and increases in the order no salt $< K^+ < Na^+ < Li^+$ and no salt $< Cl^- < Br^- < I^-$. The selectivity to furfural is also affected by salt composition, increasing in the order $K^+ < Na^+ < Li^+$ and $I^- < Br^- < Cl^-$ (as observed in initial rate studies). At 140 °C, the maximum furfural selectivity was 44% when the reaction was performed in a 5 M LiCl solution. The effects of salt on the rates of xylose dehydration and humins formation are complex and involve interactions of the salt cations and anions with both water and xylose. Metal cations disrupt the solvation of xylose by water and interact with the hydroxyl groups and ring oxygen atoms of xylose, leading to a weakening of C–O bonds. Halide anions interact to a lesser degree with water than do cations, but do interact with the positive end of hydroxyl groups on xylose, such that on average 4 Cl^- ions interact with each xylose molecule. These interactions stabilize cationic intermediates formed during the dehydration of the sugar, the degree of stabilization increasing with the nucleophilicity of the anion. Significantly, more nucleophilic anions also enhance reactions involving these intermediates to form humins, and consequently furfural selectivity decreases in the order $Cl^- < Br^- < I^-$. The addition of metal halides was also found to increase the dehydration of xylose initiated by protonation of C1OH versus C2OH groups. These findings demonstrate that alkali metal halides dissolved in water can be used to enhance the rate of xylose dehydration and the selectivity towards furfural versus humins formation. By coupling these effects with the extraction of furfural into an organic phase, high yields of furfural can be achieved.

Experimental Section

Materials

D-xylose (99%, Sigma–Aldrich), D-[5-^{18}O]-xylose (90 atom% ^{18}O, Omicron Biochemicals, Inc.), and 2-furaldehyde (furfural, 99%, Sigma–Aldrich) were used as reagents and standards (for quantification). D-xylose-1-^{13}C (99 atom% ^{13}C, Sigma–Aldrich) was used in ^{1}H and ^{13}C NMR studies.

Lithium chloride (LiCl, BioXtra, ≥99.0%–titration), lithium bromide (LiBr, anhydrous, Redi-Dri, ReagentPlus, ≥99%), lithium iodide (LiI, 99.9%–trace metals basis), sodium bromide (NaBr, puriss., 99–100.5%), sodium iodide (NaI, anhydrous, Redi-Dri, ACS reagent, ≥99.5%), potassium chloride (KCl, approx. 99%), potassium bromide (KBr, BioXtra, ≥99.0%), potassium iodide (KI, puriss., ≥99.5%), magnesium chloride ($MgCl_2$, anhydrous, ≥98%), and calcium chloride ($CaCl_2$, anhydrous, Redi-Dri, ≥97%) were purchased from Sigma–Aldrich; sodium chloride (NaCl, ≥99.0%) was purchased from Fisher Scientific. Sulfuric acid (H_2SO_4, 98%, Sigma–Aldrich) and hydrochloric acid (HCl, 37% v/v, Fisher Scientific) were used as Brønsted acid catalysts. All materials were used as purchased, without further purification or modification.

Experimental approach

All experiments were performed in 10 mL glass vials (from Sigma–Aldrich via supplier Supelco) sealed with 20 mm aluminum-crimped PTFE septa and heated using a silicon oil bath to maintain constant reaction temperature and stirring rate. In a representative xylose dehydration experiment, xylose was dissolved in 5 M brine (i.e. 5 M NaCl in nanopure water), to which HCl was added to create a solution (750 mM xylose, 50 mM H^+). A 4 mL aliquot of this solution was sealed into a 10 mL glass vial. The vial was then placed in a silicone oil bath heated to 140 °C and stirred at 600 rpm. Reaction time began after 1 min had transpired (control experiments determined this time to be necessary for the reactor to reach reaction temperature). Upon completion of the reaction, the sample was removed and quenched in an ice bath. An internal standard (1 mL of 75 mg mL^{-1} 1,6-hexanediol in water) was added and the sample centrifuged to remove all water insoluble particulates. A portion of the reaction mixture (500 μL) was diluted in a 1:1 ratio with nanopure water and taken for HPLC analysis. For reactions involving an additional organic phase, the aqueous phase volume was reduced to 1 mL and toluene (4 mL) was added prior to sealing the reaction vial. At reaction end, the organic phase was separated via centrifuging. The aqueous phase was treated as above and analyzed via HPLC, whereas a different internal standard (1 mL of 5 mg mL^{-1} guaiacol in toluene) was added to the organic phase prior to GC/MS analysis.

The influence of metal halides on the dehydration of xylose and the formation of furfural was performed using a 5 M solution of the metal halide. The choice of this concentration was based on preliminary experiments (see Figure S1 in Supporting Information) per-

formed with NaCl solutions ranging in concentration from 0 to 5 M. The natural log of the initial reaction rate versus the salt concentration revealed three distinct regimes: 1) at low concentrations (500 mM and under), rate of xylose dehydration was roughly zero-order, 2) at intermediate concentrations (500 mM to 3.5 M), the rate was roughly first-order, and 3) at high concentrations (3.5 M to 5 M), the rate was roughly zero-order. To maximize initial xylose conversion/furfural production rates, the highest salt concentration that could be achieved for all salts with respect to room-temperature solubility limits was found to be 5 M. Only salts containing Cl^-, Br^-, and I^- were used. Fluoride (F^-) salts were purposely excluded in order to avoid a reduction in the pH of the reaction solution due to the reaction of proton (from the hydrochloric acid Brønsted acid catalyst, $pK_a = -8$) with the more basic fluoride anions. Consequently, only halides of equal or lesser basicity than Cl^- were explored.

Product analysis

A Shimadzu HPLC equipped with a Phenomenex Rezex RFQ-Fast Acid H+ column (100×7.8 mm; 0.01 N H_2SO_4; 1.0 mL min^{-1}; 55 °C) and a refractive index detector (RID) was used to analyze all aqueous samples. Product quantities were determined by converting integrated HPLC peak areas into concentrations using a 7-point calibration curve generated from purchased standards.

A Varian CP-3800 Gas Chromatograph equipped with a FactorFour Capillary Column (UF-5 ms 30 m, 0.25 mm, 0.25 μm, P/N CP8944) connected to a Varian quadrupole-mass spectrometer (MS) and flame ionization detector (FID) was used to analyze all organic phase samples. After product identification by mass spectrometer, product concentrations were determined from integrated FID peak areas using a 6-point calibration curve generated from purchased standards.

A Bruker AVQ-400 console with a Bruker 9.39 T magnet was used to perform all ^{1}H (400.13 MHz) and ^{13}C (100.613 MHz) NMR experiments. ^{1}H NMR spectra were taken by using a 8.2 μs 90° pulse, whereas ^{13}C NMR spectra were taken using a standard gated decoupling pulse sequence (8.5 μs pulse width) to remove signal splitting caused by proton coupling. D-xylose-1-^{13}C labeled xylose dissolved in D_2O was used to improve signal quality in ^{13}C NMR xylose isomeric distribution studies. A Bruker AVB-400 console with a Bruker 9.39 T magnet was used to perform all ^{35}Cl (39.2 MHz) NMR experiments. ^{35}Cl-NMR spectra were taken using a 10 μs 90° pulse.

Reagent and product yields are reported as molar percentages relative to initial molar concentrations of xylose (i.e. furfural yields = moles furfural/initial moles xylose). All reported yields were typically reproducible to within a +/- 5% relative error (based upon the calculation of one standard deviation).

Acknowledgements

This work was supported by the Energy Biosciences Institute funded by BP. All NMR work was performed using equipment funded by NSF grant CHE-0130862. Special thanks to research assistance provided by Daniel Tjandra and David Doan.

Keywords: anions · carbohydrates · cations · kinetics · salt effect

[1] T. Werpy, G. Petersen, Report No. NREL/TP-510-35523, *Top Value Added Chemicals from Biomass: Vol. 1—Results of Screening for Potential Candidates from Sugars and Synthesis Gas*, National Renewable Energy Laboratory, Golden, CO, **2004**.
[2] K. J. Zeitsch, *Sugar Ser.* **2000**, *13*, 1–353.
[3] S. Bayan, E. Beati, *Chim. Ind.* **1941**, *23*, 432.
[4] a) J. N. Chheda, G. W. Huber, J. A. Dumesic, *Angew. Chem. Int. Ed.* **2007**, *46*, 7164; *Angew. Chem.* **2007**, *119*, 7298; b) G. A. Tompsett, N. Li, G. W. Huber, *Thermochemical Processing of Biomass: Conversion into Fuels, Chemicals and Power* (Ed.: Robert C. Brown), Wiley, Chichester, **2011**, pp. 223–279.
[5] B. Madhesan, E. R. Sacia, A. T. Bell, *ChemSusChem* **2014**, *7*, 1078.
[6] a) G. W. Huber, J. N. Chheda, C. J. Barrett, J. A. Dumesic, *Science* **2003**, *300*, 2075; b) G. W. Huber, J. A. Dumesic, *Catal. Today* **2006**, *111*, 119.
[7] C. Moreau, R. Durand, D. Peyron, J. Duhamet, P. Rivalier, *Ind. Crops Prod.* **1998**, *7*, 95.
[8] a) G. W. Huber, S. Iborra, A. Corma, *Chem. Rev.* **2006**, *106*, 4044; b) C. E. Wyman, S. R. Decker, M. E. Himmel, J. W. Brady, C. E. Skopec, L. Viikari, *Polysaccharides: Structural Diversity and Functional Versatility, Vol. 2* (Ed.: S. Dumitriu), Marcel Dekker, New York, **2005**, pp. 995–1033.
[9] R. Weingarten, J. Cho, W. C. Conner, G. W. Huber, *Green Chem.* **2010**, *12*, 1423.
[10] J. N. Chheda, Y. Roman-Leshkov, J. A. Dumesic, *Green Chem.* **2007**, *9*, 342.
[11] a) E. O. Eisen, J. Joffe, *J. Chem. Eng. Data* **1966**, *11*, 480; b) E. I. Gürbüz, S. G. Wettstein, J. A. Dumesic, *ChemSusChem* **2012**, *5*, 383; c) B. Saha, N. S. Mosier, M. M. Abu-Omar, *Advances in Plant Biology: Plants and Bio-Energy, Vol. 4* (Eds.: M. McCann, M. S. Buckeridge, N. C. Carpita), Springer, New York, **2013**, pp. 267–276; d) Y. Román-Leshkov, J. A. Dumesic, *Top. Catal.* **2009**, *52*, 297.
[12] a) G. Marcotullio, W. D. Jong, *Green Chem.* **2010**, *12*, 1739; b) G. Marcotullio, W. D. Jong, *Carbohydr. Res.* **2011**, *346*, 1291.
[13] T. W. G. Solomons, C. B. Fryhle, *Organic Chemistry, 8th ed.*, Wiley, Hoboken, NJ, **2004**.
[14] a) W. J. Hamer, Y. C. Wu, *J. Phys. Chem. Ref. Data* **1972**, *1*, 1047; b) R. N. Goldberg, R. L. Nuttall, *J. Phys. Chem. Ref. Data* **1978**, *7*, 263.
[15] a) C. D. Cappa, J. D. Smith, K. R. Wilson, B. M. Messer, M. K. Gilles, R. C. Cohen, R. J. Saykally, *J. Phys. Chem. B* **2005**, *109*, 7046; b) J. D. Smith, R. J. Saykally, P. L. Geissler, *J. Am. Chem. Soc.* **2007**, *129*, 13847.
[16] J. Israelachvili, *Intermolecular and Surface Forces, 2nd ed.*, Academic Press, London, UK, **1991**.
[17] J. P. Mikkola, R. Sjoholm, T. Salmi, P. Maki-Arvela, *Catal. Today* **1999**, *48*, 73.
[18] S. J. Angyal, *Adv. Carbohydr. Chem. Biochem.* **1989**, *47*, 1.
[19] P. Ortiz, J. Fernandez-Bertran, E. Reguera, *Spectrochim. Acta Part A* **2005**, *61*, 1977.
[20] a) R. C. Remsing, R. P. Swatloski, R. D. Rogers, G. Moyna, *Chem. Commun.* **2006**, 1271; b) J. J. Falke, R. J. Pace, S. I. Chan, *J. Biol. Chem.* **1984**, *259*, 6472; c) J. J. Falke, K. J. Kanes, S. I. Chan, *J. Biol. Chem.* **2005**, *260*, 9545.
[21] B. Danon, G. Marcotullio, W. de Jong, *Green Chem.* **2014**, *16*, 39.
[22] M. R. Nimlos, X. Qian, M. Davis, M. E. Himmel, D. K. Johnson, *J. Phys. Chem. A* **2006**, *110*, 11824.
[23] X. H. Qian, M. R. Nimlos, D. K. Johnson, M. E. Himmel, *Appl. Biochem. Biotechnol.* **2005**, *124*, 989.
[24] M. J. Antal, T. Leesomboon, W. S. Mok, G. N. Richards, *Carbohydr. Res.* **1991**, *217*, 71.

Received: October 20, 2014
Published online on January 13, 2015